[CANCER RESEARCH 61, 6583–6591, September 1, 2001]

ErbB2/*neu* Kinase Modulates Cellular $p27^{Kip1}$ and Cyclin D1 through Multiple Signaling Pathways[1]

Anne E. G. Lenferink,[2] Dagmar Busse,[3] W. Michael Flanagan,[4] F. Michael Yakes, and Carlos L. Arteaga[5]

Departments of Medicine [A. E. G. L., D. B., F. M. Y., C. L. A.] and Cell Biology [C. L. A.], Vanderbilt University School of Medicine, Department of Veteran Affairs Medical Center [C. L. A.], and Vanderbilt Ingram Cancer Center [C. L. A.], Nashville, Tennessee 37232, and Gilead Sciences, Foster City, California 94404 [W. M. F.]

ABSTRACT

It is well established that ErbB1 and ErbB2 can cooperate in mammary epithelial cell transformation. Therefore, to understand how ErbB1/ErbB2 signaling contributes to this process, we used the ErbB kinase inhibitor AG1478 in ErbB2-dependent BT-474 and SKBR-3 human breast cancer cells. These cells overexpress ErbB2 and also display moderate levels of ErbB1. Treatment with AG1478 resulted in rapid ErbB2 dephosphorylation, reversible G_1 arrest, and interruption of constitutive mitogen-activated protein kinase (MAPK) and phosphatidylinositol 3-kinase (PI3K)/Akt signaling. Consequently, both MAPK-dependent transcription of cyclin D1 and phosphorylation of the cyclin-dependent kinase (Cdk) inhibitor p27 were inhibited. The inhibition of PI3K/Akt resulted in increased activity of glycogen synthase kinase-3β, which phosphorylated cyclin D1, potentially reducing its steady-state levels. The loss of cyclin D1 reduced the amount of cyclin D1/Cdk4 complexes that can sequester p27 in the cytosol. This plus the reduced phosphorylation of p27 by MAPK enhanced the stability of p27 that associated with nuclear Cdk2 at high stoichiometry and inhibited its kinase activity. Antisense p27 oligonucleotides decreased p27 levels and abrogated the G_1 arrest induced by AG1478. Similarly, infection with an adenovirus encoding inducible cyclin D1 also counteracted the antiproliferative effect of AG1478. These data imply that: (*a*) modulation of both p27 and cyclin D1 are required for the growth arrest that results from blockade of the ErbB2 kinase; and (*b*) ErbB2 overexpressing cells use both MAPK and PI3K/Akt to modulate p27 and cyclin D1 and, hence, subvert the G_1-to-S transition.

INTRODUCTION

The ErbB receptors are involved in development, cell proliferation, differentiation, lineage determination, and oncogenesis (1–3).The ErbB receptor family consists of four transmembrane tyrosine kinases: ErbB1/EGFR,[6] ErbB2/*neu*, ErbB3, and ErbB4. The ectodomain of each ErbB1, ErbB3, and ErbB4 interacts with a specific set of ligands, whereas no ligand has been identified thus far for the (orphan) ErbB2 receptor (3, 4). Nonetheless, ErbB2 can be activated by any of the other ligand-activated ErbB coreceptors. Upon ligand binding to the ectodomain of ErbB1, ErbB3, or ErbB4, these receptors preferentially recruit ErbB2 into a heterodimeric complex in which the ErbB2 kinase can modulate receptor internalization and prolong signal transduction (5–7). Inactivation of ErbB2 function has been shown to impair signaling induced by the coreceptor ligands EGF and Neu differentiation factor, confirming the critical role of ErbB2 in the cellular effects of the ErbB receptor network (8, 9). Finally, overexpression of ErbB2 results in epithelial cell transformation, and high levels in tumor tissues predict for poor patient prognosis in several human cancers (10).

The activation of ErbB receptors results in the activation of a large network of independent signaling pathways that mediate enhanced proliferation and/or survival (2, 3). Overexpression of these signal transduction programs coupled with mutations in cell cycle regulators in tumor cells results in the subversion of cell cycle checkpoints and dysregulated cell proliferation (11, 12). In nontransformed mammalian cells, regulation of the cycle machinery is strictly controlled by several Cdks. The activity of these molecules is regulated by several mechanisms: (*a*) phosphorylation and dephosphorylation (reviewed in Ref. 13); (*b*) the association with specific regulatory cyclins (14); and (*c*) by the interaction with specific Cdk inhibitors (13, 15). On the basis of their structure and cellular targets, Cdk inhibitors can be assigned to two families: (*a*) the INK4 proteins that inhibit Cdk4 and Cdk6 (INK4a–d); and (*b*) the more broadly acting Cip/Kip family, which inhibits the catalytic subunits of the cyclin A-, D- and E-dependent kinases. The Cip/Kip family includes $p21^{Cip1}$, $p27^{Kip1}$, and $p57^{Kip2}$ (13, 15). Progression through the G_1-S transition is mainly regulated through the sequential activation of Cdk4, Cdk6, and Cdk2. These kinases are activated by D-type cyclins in mid-to-late G_1 and by cyclin E in late G_1 (13). Cip/Kip inhibitors bind all Cdks and may prevent their activation by Cdk-activating kinases or directly inhibit their kinase activity *per se*. One of the Cip/Kip inhibitory molecules is p27, which was originally discovered as a Cdk inhibitory activity induced by extracellular antimitogenic signals (16, 17). Although p27 can interact with and inhibit recombinant cyclin D/Cdk complexes *in vitro*, it seems to be most effective in antagonizing the activity of cyclin E/Cdk2 complexes *in vivo*. By contrast, p27 seems to be required for the assembly and function of cyclin D/Cdk4 complexes in intact cells (18).

In this study, we present evidence that ErbB2 reversibly reduces p27 and increases cyclin D1 levels through both MAPK and PI3K/Akt signaling, with neither of these pathways being dispensable for cell cycle progression. In turn, ErbB2 blockade eliminates the coordinated MAPK and PI3K/Akt inputs on p27 and cyclin D1, resulting in stabilization of p27, reduction in cyclin D1 and Cdk4, loss of Cdk2 function, and cell cycle arrest.

MATERIALS AND METHODS

Cell Lines, Kinase Inhibitors, and Antibodies. The MCF-7/ErbB2 clone 11, MCF-7/ErbB2 clone 18, and MCF-7/neo cells (19) were provided by C. K. Osborne (Baylor College of Medicine). BT-474 and SKBR-3 cells were obtained from the American Type Culture Collection (Manassas, VA). All cells were maintained in IMEM (Life Technologies, Inc., Rockville, MD) containing 10% FCS (Atlanta Biologicals, Norcross, GA) at 37°C in a humidified, 5% CO_2 atmosphere. AG1478 was provided by L. K. Shawver (Sugen,

Received 4/25/01; accepted 7/5/01.

The costs of publication of this article were defrayed in part by the payment of page charges. This article must therefore be hereby marked *advertisement* in accordance with 18 U.S.C. Section 1734 solely to indicate this fact.

[1] This work was supported by NIH Grant R01 CA80195 (to C. L. A.), a Department of Veteran Affairs Clinical Investigator Award (to C. L. A.), and Vanderbilt-Ingram Cancer Center Support Grant CA68485. D. B. was supported by the Robert-Bosch Foundation (Stuttgart, Germany). A. E. G. L. is the recipient of a fellowship award from the Susan G. Komen Foundation.

[2] Present address: Biotechnology Research Institute, National Research Council, 6100 Royalmount Avenue, Montreal, Quebec, H4P 2R2 Canada.

[3] Present address: Dr. Margarete Fischer-Bosch-Institut für Klinische Pharmakologie, 70376 Stuttgart, Germany.

[4] Present address: Sunesis Pharmaceuticals, 3696 Haven Avenue, Suite C, Redwood City, CA 94063.

[5] To whom requests for reprints should be addressed, at Division of Oncology/Vanderbilt University, 777 Preston Research Building, Nashville, TN 37232-6307. Phone: (615) 936-3524; Fax: (615) 936-1790; E-mail: carlos.arteaga@mcmail.vanderbilt.edu.

[6] The abbreviations used are: EGFR, epidermal growth factor receptor; Cdk, cyclin-dependent kinase; MAPK, mitogen-activated protein kinase; PI3K, phosphatidylinositol 3-kinase; IMEM, Improved Minimal Essential Medium; PMSF, phenylmethylsulfonyl fluoride; tet, tetracycline; GST, glutathione *S*-transferase; GSK-3β, glycogen synthase kinase-3β; MBP, myelin basic protein; Luc, luciferase; HH1, histone H1; MMTV, mouse mammary tumor virus; TGF, transforming growth factor; Erk, extracellular signal-regulated kinase; MEK, MAPK kinase.

Inc.); U-0126 (20) was from Calbiochem (San Diego, CA); and LY294002 (21) was from Biomol Research (Plymouth Meeting, PA). For immunoblot analysis and immunoprecipitations, the following antibodies were used: ErbB1, GSK-3β, and p27 (Transduction Laboratories, Lexington, KY); ErbB2/neu (Neomarkers, Freemont, CA); P-Tyr (Upstate Biotechnology, Lake Placid, NY); Rb and cyclin D1 (PharMingen, San Diego, CA); MAPK, P(Ser9)-GSK-3β, Akt, and P(Ser473)-Akt (New England BioLabs, Beverly, MA); P-MAPK (Promega Corp., Madison, WI); cyclin E, cyclin E/Cdk2 and Cdk4 (Santa Cruz Biotechnology, Santa Cruz, CA); c-jun, a gift from T. Curran (St. Jude Children's Hospital); and α-tubulin (Amersham Pharmacia, Piscataway, NJ). Protein in cell lysates was measured by bicinchoninic acid (Pierce, Rockford, IL) or Bio-Rad (Hercules, CA) assays.

Flow Cytometric Analysis. Proliferating BT-474 cells in IMEM/10% FCS were treated with AG1478. Cells were harvested by trypsinization, and their nuclei were labeled with propidium iodide as described previously (22). Cells were filtered through a 95-μm pore size nylon mesh (Small Parts, Inc., Miami Lakes, FL), and a total of 15,000 nuclei were analyzed in a FACS/Calibur Flow Cytometer (Becton Dickinson, Mansfield, MA). DNA histograms were modeled off-line using Modfit-LT-Software (Verity, Topsham, ME).

Immunoblot Analysis and Immunoprecipitation. Subconfluent monolayers ($\cong$50%) were treated for 24 h with AG1478, LY294002, or U0126. Cells were washed twice with ice-cold PBS, scraped in EBC lysis buffer [50 mM Tris-HCl (pH 8.0), 120 mM NaCl, 0.5% NP40, 100 mM NaF, 200 μM Na_3VO_4, and 10 μg/ml each aprotinin, leupeptin, PMSF, and pepstatin], and incubated for 20 min at 4°C while rocking. Lysates were cleared by centrifugation (10 min at 12,000 rpm, 4°C). For immunoblot analysis, 75 μg of total protein were resolved by SDS-PAGE and transferred to nitrocellulose membranes. Membranes were blocked with TBS-T [25 mM Tris-HCl, 150 mM NaCl (pH 7.5), and 0.05% Tween 20] containing 5% nonfat milk and incubated overnight at 4°C with primary antibody in TBS-T/1% nonfat milk. Blots were washed in TBS-T and incubated with the appropriate horseradish peroxidase-linked IgG (Amersham Pharmacia), and immunoreactive bands were detected by chemiluminescence (Roche Molecular Biochemicals, Indianapolis, IN). For immunoprecipitations, 1 mg (from whole cell lysates) or 500 μg (from cytosolic and nuclear fractions) of total protein were incubated overnight with primary antibody at 4°C; protein A-Sepharose (Sigma Chemical Co.; 1:1 slush in PBS) was then added for 2 h at 4°C while rocking. The precipitates were washed four times with ice-cold PBS, resuspended in 6$\times$ Laemmli sample buffer, and resolved by SDS-PAGE followed by immunoblot analysis.

Studies with Antisense Oligonucleotides and Cyclin D1 Adenovirus. The sequences of the p27 antisense and the mismatch control oligonucleotides were TGG CTC TCX TGC GCC (GS5413) and TGG CTC XCT TGC GCC (GS5585), respectively (23). The oligonucleotides (final concentration, 30 nM) were heated for 5 min at 65°C in serum-free medium to denature their secondary structure, then mixed with 2 μg/ml cytofectin GS3815 (Gilead Sciences) in 400 ml of serum-free minimal Eagle's medium (MEM; Life Technologies, Inc.) in polystyrene tubes, and incubated at room temperature for 10 min. Thereafter, 1.6 ml of IMEM/10% FCS were added, and the resulting 2 ml of "transfection volume" were placed on each 60-mm tissue culture dish with BT-474 cells. Control cells were incubated under identical conditions with 400 ml of MEM (containing 2 μg/ml cytofectin) + 1.6 ml IMEM. After 5 h, 2 ml of IMEM/10% FCS were added to each dish, and the cells were incubated in the absence or presence of AG1478 for 20 additional h. Cells were finally harvested and subjected to Rb and p27 immunoblot procedures and flow cytometric analysis.

To induce expression of cyclin D1, we used an adenoviral vector encoding the human *cyclin D1* gene (Ad-D1; provided by T. Meeker, University of Kentucky, Lexington, KY). *Cyclin D1* gene expression is achieved by coinfection with a helper virus that is inhibited by tetracycline (Ad-tTA; Ref. 24). BT-474 cells (10^6) in 100 μl of Optimem (Life Technologies, Inc.)/2% FCS were incubated for 2 h at 37°C with both Ad-D1 and Ad-tTA, each at an multiplicity of infection of 200:1. Cells were then plated in IMEM/10% FCS $\pm$ 10 nM tet. In the absence of tet, high cyclin D1 expression was evident 48 h later. AG1478 was added for the second 24-h period, after which cells were harvested and prepared for immunoblot or cell cycle analyses as described above.

Cell Fractionation. After washes and scrapping in PBS, cells were pelleted by centrifugation (5 min, 12,000 rpm, 4°C) and incubated in a hypotonic buffer [10 mM HEPES (pH 7.2), 10 mM KCl, 1.5 mM $MgCl_2$, 0.1 mM EGTA, 20 mM NaF, 100 μM Na_3VO_4, and 10 μg/ml of each aprotinin, pepstatin, PMSF, and leupeptin] for 30 min at 4°C while rocking. Cells were broken using a Dounce homogenizer (30 strokes), after which nuclei were pelleted by centrifugation (10 min, 3500 rpm, 4°C). The nuclei-free supernatant was subjected to a second 100,00 $\times$ *g* centrifugation for 45 min at 4°C to separate membrane (pellet) from cytosolic (supernatant) fractions. Nuclear pellets (above) were resuspended in nuclear lysis buffer [10 mM Tris-HCl (pH 7.5), 150 mM NaCl, 5 mM EDTA, and 1% Triton X-100] and incubated for 1 min in a sonicating water bath, followed by a 30-min incubation at 4°C while rocking. Twenty μg of total cytosolic and nuclear protein were analyzed by immunoblot.

Endogenous p27 *in Vitro* Degradation Assay. BT-474 cells were scrapped in p27 degradation buffer [20 mM Tris-HCl (pH 7.6), 2 mM DTT, 0.25 mM EDTA, and 10 μg/ml leupeptin and pepstatin]. Cell suspensions were freeze-thawed three times in liquid N_2 and cleared by centrifugation (10 min, 12,000 rpm, 4°C). Twenty μg of total protein (supernatant) were incubated in a total volume of 30 μl of p27 degradation buffer containing 5 mM $MgCl_2$, 10 mM creatine-PO_4, 10 μg/ml creatine kinase (both Roche Molecular Biochemicals), and 0.5 mM ATP (final concentration). Samples were incubated at 30°C for 0.5–20 h, and the degradation reaction was terminated by adding 6$\times$ Laemmli sample buffer. The level of p27 in the samples was determined by immunoblot. Densitometric analysis of the immunoreactive bands was carried out using NIH Image Software (Research Services Branch, NIH, Bethesda, MD).

Recombinant Protein Purification. Expression and purification of His-tagged recombinant wild-type and mutant (Thr-187 replaced by Ala) p27 (provided by M. Pagano, New York University, New York, NY) was performed as described previously (25). Briefly, bacteria containing the p27 plasmids were grown overnight at 37°C (250 rpm) in Luria Broth medium and induced with isopropyl-1-thio-β-D-galactopyranoside (Fisher Biotech, Fair, NJ) for 4 h. Bacterial pellets were resuspended in lysis buffer [300 mM NaCl, 50 mM Na_2PO_4 (pH 8.0), 1% Tween 20, and 10 μg/ml of each aprotinin, leupeptin, PMSF, soybean trypsin inhibitor, *N*-tosyl-L-phenylalanine chloromethyl ketone, *N*α-*p*-tosyl-L-lysine chloromethyl ketone (Sigma Chemical Co.), NaF, and Na_3VO_4] and lysed by sonication. Lysates were cleared by centrifugation (20 min, 10,000 rpm, 4°C), and the supernatants were incubated with Ni-NTA Agarose (Qiagen, Inc., Valencia, CA). Recombinant proteins were eluted in a stepwise fashion using wash buffer [300 mM NaCl, 50 mM Na_2PO_4 (pH 6.0), 10% glycerol, 1% Tween 20, and protease/phosphatase inhibitors] containing 100, 250, 500, or 1000 mM imidazole. The fractions containing recombinant proteins were pooled, dialyzed overnight against PBS, and stored at $-$80°C. GST-cyclin D1 fusion protein (GST fused to the last 41 COOH-terminal amino acids of cyclin D1; a gift from C. J. Sherr, St. Jude Children's Hospital, Memphis, TN) was bacterially expressed and purified as described by Diehl *et al.* (26). Bacteria were grown overnight in Luria Broth medium (37°C, 250 rpm), induced the next day for 4 h with 1 mM isopropyl-1-thio-β-D-galactopyranoside, and collected by centrifugation. Bacterial pellets were sonicated in lysis buffer [20 mM Tris-HCl (pH 7.5), 150 mM NaCl, 0.5% NP40, and 1 mM PMSF], cleared by centrifugation (20 min, 10,000 rpm, 4°C), and incubated with glutathione-coupled-agarose (1:1 slush in PBS; Sigma Chemical Co.) for 1 h at 4°C. GST-cyclin D1 fusion proteins were eluted from the glutathione-agarose beads using GSK-3β kinase buffer (below) containing 4 mM reduced glutathione (Sigma Chemical Co.).

***In Vitro* Kinase Assays.** Cells were washed with ice-cold PBS and lysed in EBC buffer. One mg of total protein was precipitated overnight at 4°C with MAPK, Cdk2, or GSK-3β antibodies and protein A-Sepharose. Immunoprecipitates were washed four times with ice-cold PBS, two times with kinase buffer [Cdk2 kinase buffer: 50 mM HEPES (pH 7.5), 10 mM $MgCl_2$, 2.5 mM EGTA, 1 mM DTT, 0.1 mM NaF, 0.1 mM Na_3VO_4, and 1 mM ATP; MAPK kinase buffer: 30 mM HEPES (pH 7.4), 15 mM $MgCl_2$, and 1 mM ATP; GSK-3β kinase buffer: 50 mM HEPES (pH 7.5), 10 mM $MgCl_2$, 1 mM EGTA, 1 mM DTT, 1 mM PMSF, 0.4 mM NaF, 0.4 mM Na_3VO_4, and 1 mM ATP], and finally resuspended in 20 μl of its respective kinase buffer. Cdk2 precipitates were assayed for their kinase activity by adding 1 μg of HH1 (Roche Molecular Biochemicals), and MAPK activity, by adding 5 μg of MBP (Upstate Biotechnology). Cdk2 or MAPK precipitates were also incubated with 10 μg of His-tagged wild-type or T187A p27 proteins. GSK-3β kinase activity was determined against 5 μg of recombinant GST-cyclin D1. Kinase reactions were performed in a final volume of 30 μl in the presence of 5 μCi of [γ-^{32}P]ATP (specific activity, 3000 Ci/mmol; Amersham Pharmacia) for 45 min at 30°C,

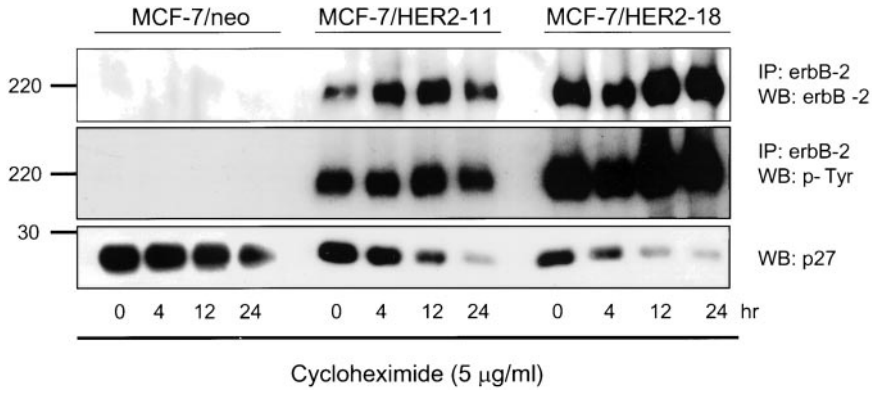

Fig. 1. p27 protein stability is reduced by ErbB2 overexpression. MCF-7/neo, MCF-7/ErbB2–11, and MCF-7/ErbB2–18 cells were grown in IMEM/10% FCS until reaching 50% confluency. Cells were then replenished with fresh medium containing 5 μg/ml cycloheximide. At the indicated times, the cells were washed with ice-cold PBS and solubilized in EBC buffer. One mg of protein per sample was subjected to immunoprecipitation (*IP*) with ErbB-2 antibodies. Immune complexes were next resolved by SDS-PAGE and subjected to Western blot (*WB*) procedures for ErbB2 and P-Tyr. Where indicated, the p27 content in 50 μg of total protein per lane was analyzed by immunoblot. *Left*, molecular weights in thousands.

25 min at 25°C, or 30 min at 30°C for Cdk2, MAPK, and GSK-3β, respectively.

Cyclin D1/Luciferase Reporter Assays. BT-474 cells in IMEM/10% FCS were seeded in 24-well plates (2×10^5 cells/well). Twenty-four h later, the cells were transfected with 250 ng of pGL3 vector containing the cyclin D1 promoter (a gift from L. Sealy, Vanderbilt University, Nashville, TN) and 1 ng of pRL-CMV construct (Promega) using Fugene-6 Transfection Reagent (Roche Molecular Biochemicals). Twenty-four h after transfection, 10 μM AG1478 or 5 μM U0126 were added to the cells. After a 24-h incubation with these inhibitors, the cells were washed with PBS, lysed, and analyzed for firefly Luc and *Renilla reniformis* Luc activities using the Dual Luciferase Reporter Assay system (Promega) according to the manufacturer's instructions in a Monolight 2010 luminometer (Analytical Luminescence Laboratory, San Diego, CA). Luc activity was normalized to *Renilla reniformis* Luc and expressed as fold-induction above control.

RESULTS

Overexpression of ErbB2 Increases the Turnover of p27. We initially examined the effect of forced expression of ErbB2 on the half-life of p27 in MCF-7 cells that contain a single copy of the *ErbB2* gene. MCF-7/ErbB2 clones 11 and 18 exhibited high levels of total and phosphorylated ErbB2, whereas these were undetectable in MCF-7/neo cells (Fig. 1). Treatment with the protein synthesis inhibitor cycloheximide revealed a half-life for p27 of approximately 12 and 4 h in clones 11 and 18, respectively, correlating inversely with the levels of phosphorylated ErbB2. Levels of the Cdk inhibitor were minimally reduced at 24 h in MCF-7/neo cells treated with cycloheximide (Fig. 1), suggesting that overexpression of ErbB2 increased the turnover of p27. The steady-state levels of cyclin D1 protein were similar in all three cell lines (not shown).

AG1478 Induces Reversible Inhibition of the ErbB2 Kinase and G_1 Arrest. To study ErbB2-driven cell cycle progression, we used BT-474 and SKBR-3 breast cancer cells, which exhibit *ErbB2* gene amplification (27) and are ErbB2 dependent. To block ErbB2 signaling, we used the quinazoline AG1478, which inhibits the ErbB1 and ErbB2 kinases *in vitro* with an IC_{50} of 3 nM (28) and 1.4 μM, respectively.[7] Although relatively specific for ErbB1 at low concentrations, AG1478 can induce inactive, unphosphorylated ErbB1/ErbB2 heterodimers (29), thus inhibiting ErbB2 function and the colony survival of these cells with an IC_{50} <1 μM (22).[8] In exponentially growing BT-474 and SKBR-3 cells, AG1478 eliminated ErbB2 phosphorylation (within 30 min) without altering ErbB2 protein levels. The increase in G_1 and a reduction in the S-phase fraction occurred after 28 h of treatment with AG1478. At this time, Rb was unphosphorylated, cyclin D1 was down-regulated, and p27 levels were increased (Fig. 2). Within 3 h (in BT-474) and <8 h (in SKBR-3) of removal of AG1478, ErbB2 was phosphorylated and cyclin D1 levels were markedly increased. However, the cells remained in G_1 for >24 h after removal of AG1478 and reentered into S-phase at 48 h, the time at which Rb was hyperphosphorylated and p27 levels were down-regulated (Fig. 2). In SKBR-3 cells, p21 was only detectable after removal of AG1478 (Fig. 2*B*). The content of cyclin A was not altered in either cell line (data not shown). These results suggested that AG1478 reversibly inhibited the ErbB2 kinase *in vivo* and that p27 was probably limiting for cell cycle progression.

Up-Regulation of p27 Partially Mediates AG1478-induced G_1 Arrest. To determine whether p27 played a role in the cell cycle arrest upon blockade of ErbB2, we used an antisense oligonucleotide approach. Cytofectin-mediated delivery of G-clamp modified, 15-mer antisense p27 phosphorothioates blocked the increase in p27 and the hypophosphorylation of Rb induced by 1–5 μM AG1478, whereas mismatch controls or cytofectin alone did not (Fig. 3*A*). In cells treated with cytofectin alone or mismatch oligonucleotides, 1–5 μM AG1478 induced an increase in the G_1 fraction (from 71 to 87; 84%) and a decrease in the proportion of cells in S-phase (from 18 to 6; 11%). These did not occur in cells preincubated with antisense p27 oligonucleotides (Fig. 3*B*) and in which the levels of p27 had been down-regulated. Cdk2 and Cdk4 protein levels were not altered by either oligonucleotide (not shown). Similar results were obtained three

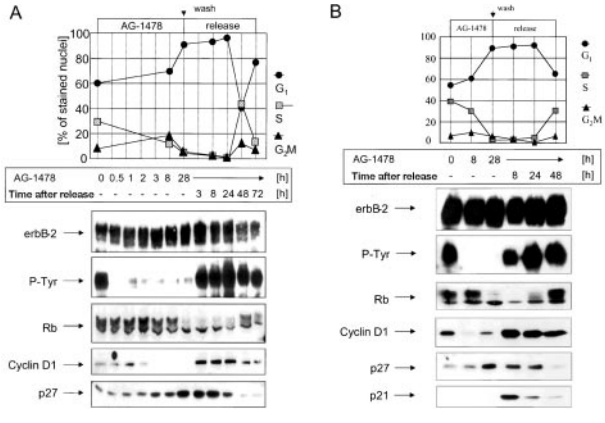

Fig. 2. Time-dependent, reversible effect of AG1478. Subconfluent BT-474 **(*A*)** and SKBR-3 cells **(*B*)** were incubated in IMEM/10% FCS containing 5 μM AG1478 for up to 28 h. At the indicated times, cells were either trypsinized or lysed in EBC buffer and evaluated for their cell cycle distribution and for ErbB2, P-Tyr, Rb, cyclin D1, p27, and p21 content. At 28 h, some of the monolayers were washed twice with PBS and replenished with fresh IMEM/10% FCS without the kinase inhibitor [*release* (*top panel*)]. At the indicated times after the removal of AG1478, cells were harvested and subjected to the same flow cytometric and immunoblot procedures performed previously. Each *lane* contains 50 μg of total protein.

[7] L. K. Shawver, personal communication.
[8] C. L. Arteaga, unpublished data.

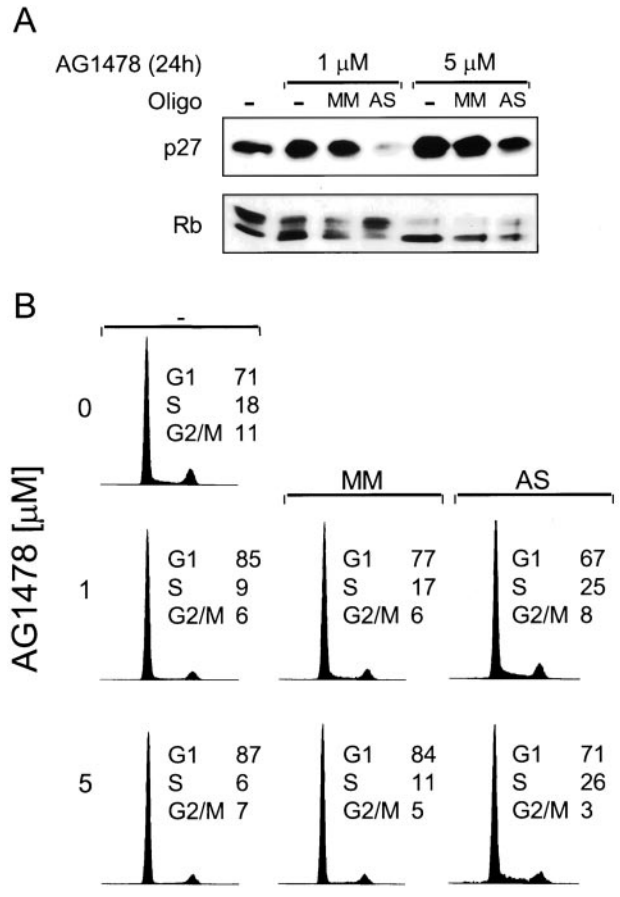

Fig. 3. Abrogation of quinazoline-mediated G_1 arrest with antisense p27 oligonucleotides. *A*, BT-474 cells were left untreated (−) or transfected with 30 nM mismatch (*MM*) or antisense (*AS*) phosphorothioate p27 oligonucleotides in the presence of 2 μg/ml cytofectin. To control for nonspecific effects of cytofectin, cells treated with neither oligonucleotide were still treated with cytofectin alone (*Lanes 2* and *5*). The cells were then exposed to 0, 1, or 5 μM AG1478 for 24 h. At this time, the cells were harvested, lysed in EBC buffer, and tested in p27 and Rb immunoblot procedures. Note that, at both concentrations, treatment with AG1478 increased the ratio of unphosphorylated:phosphorylated Rb, except in cells treated with antisense p27. *B*, identically treated cells were trypsinized, their nuclei were labeled with propidium iodide, and DNA histograms were generated by flow cytometry of 15,000 labeled nuclei. In cells treated with antisense p27 but no AG1478, S-phase was 29% (not shown).

times, suggesting a critical role for p27 in the G_1 arrest that follows blockade of the ErbB2 kinase.

ErbB2 Overexpression Induces Reversible Activation of MAPK and PI3K/Akt. We next examined whether cell cycle regulatory pathways are up-regulated by ErbB2 and whether these were sensitive to blockade of ErbB2. In all three lines, ErbB1 was undetectable by immunoblot (Fig. 4), consistent with their reported low levels of EGF receptors as measured by more sensitive methods in other studies (30, 31). On the other hand, ErbB2 was only detectable in the MCF-7/ErbB2–18 and BT-474 cells but not in MCF-7/neo cells. The ErbB2 band comigrated with a M_r 180,000 P-Tyr band in MCF-7/ErbB2–18 and BT-474 cells; this band was eliminated by treatment with AG1478, suggesting that ErbB2 kinase activity was constitutive in these cell lines. The content of both total MAPK and total Akt were similar in all three cell lines. However, active MAPK and active Akt as measured by antibodies specific for phospho-ERK1/2 and phospho-Ser473 Akt, respectively, were higher in MCF-7/ErbB2–18 and BT-474 than in MCF-7/neo cells. A 24-h treatment with 10 μM AG1478 reduced both active MAPK and active Akt without changes in total MAPK and total Akt. To follow the AG1478 mediated down-regulation of cyclin D1, we examined Cdk levels. Cdk2 protein levels were similar in all three cell lines. However, Cdk4 levels were lower in the two ErbB2-overexpressing lines and were further reduced by inhibition of ErbB2 with AG1478 (Fig. 4).

Interruption of ErbB2 Signaling alters p27/Cdk Stoichiometry, Cyclin E/Cdk2 and MAPK Activities, and p27 Stability. p27 functions as a direct inhibitor of the catalytic activity of Cdks (13, 15). Thus, we examined whether the cell cycle arrest induced by inhibition of ErbB2 (Fig. 2) was explained by modulation of p27/Cdks stoichiometry. In proliferating BT-474 cells, p27 coprecipitated with both Cdk4 and Cdk2, with higher levels of p27 precipitating with Cdk4 than with Cdk2 antibodies (Fig. 5*A*). Upon interruption of ErbB2 signaling with AG1478, the association of Cdk2 with p27 was markedly increased with significant inhibition of the amount of p27 that precipitated with Cdk4 antibodies or *vice versa*. Cdk2 protein levels were not altered, whereas Cdk4 levels were markedly reduced by AG1478, accounting in part for the diminished interaction with p27 (Fig. 5*A*). Because p27 can either inhibit cyclin E/Cdk2 activity or serve as a substrate for Cdk2-mediated phosphorylation, we performed Cdk2 *in vitro* assays using HH1 and recombinant p27 as

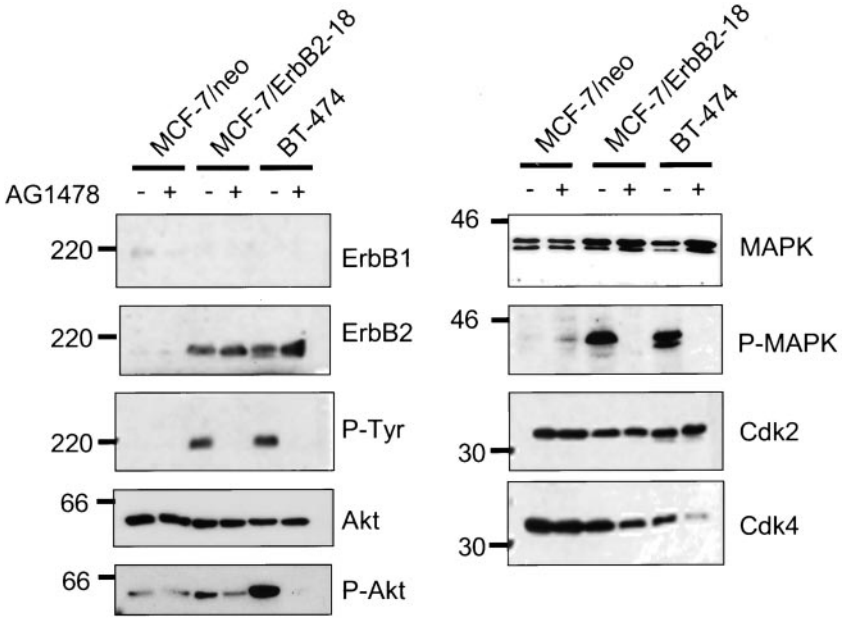

Fig. 4. ErbB2 overexpression activates MAPK and Akt. MCF-7/neo, MCF-7/ErbB2–18, and BT-474 cells were incubated for 24 h in the absence (−) or presence (+) of 10 μM AG1478. Seventy-five μg of total cell protein were resolved by SDS-PAGE and analyzed by immunoblot using antibodies against ErbB1 (EGFR), ErbB2, P-Tyr, Akt, P-Akt, MAPK, P-MAPK, Cdk2, and Cdk4. *Left* of each *panel*, molecular weights in thousands.

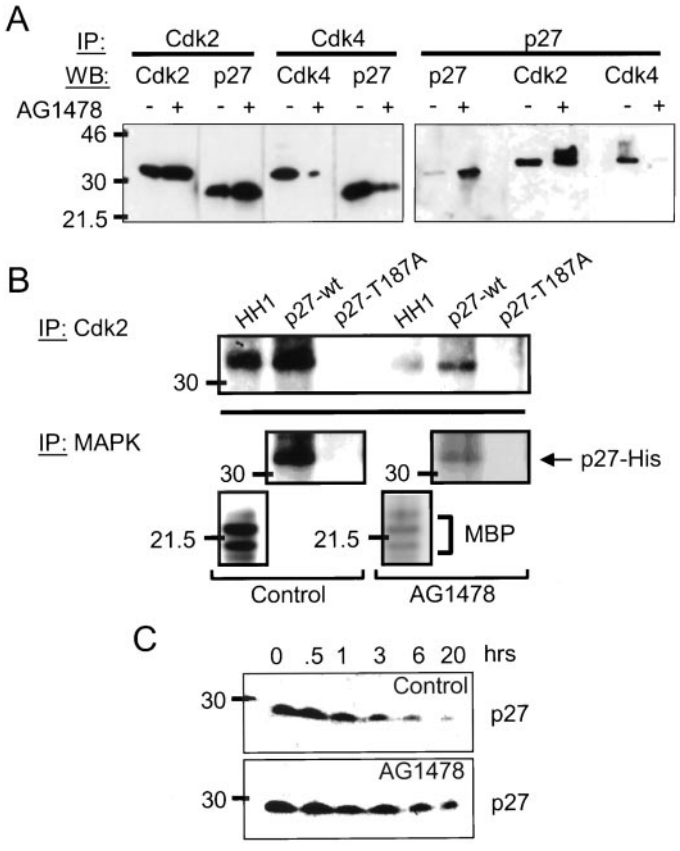

Fig. 5. Inhibition of ErbB2 reduces the association of p27 with Cdk4, blocks Cdk2 and MAPK activities, and stabilizes p27. *A*, Cdk2 and Cdk4 (*left panel*) and p27 (*right panel*) were immunoprecipitated from 1 mg of total protein from BT-474 cells that had been incubated for 24 h with or without 10 μM AG1478. Immune complexes were divided equally, and each aliquot was subjected to immunoblot analyses for Cdk2, Cdk4, and p27. *IP*, immunoprecipitation; *WB*, Western blot. *B*, Cdk2 (*top*) and MAPK (*bottom*) *in vitro* kinase assays. Cdk2 or MAPK were precipitated from 1 mg of total protein from AG1478-treated (24 h) and untreated BT-474 cells. The precipitated kinase activity was determined using HH1 (for Cdk2), MBP (for MAPK), and wild-type and T187A p27 (for both Cdk2 and MAPK) as substrates. HHI and the recombinant p27 proteins migrate at the same level (M_r ≈32,000). *IP*, immunoprecipitation. *C*, degradation of endogenous p27. Twenty μg of total protein from AG1478 treated (24 h) or control BT-474 cells were incubated for variable times at 30°C in a kinase buffer containing creatine, creatine kinase, and ATP. The p27 content of the samples was determined by immunoblot. *Left* of each *panel*, molecular weights of immunoreactive bands.

kinase substrates. Fig. 5*B* shows that inhibition of ErbB2 reduced basal Cdk2 activity against HH1 and wild-type p27 in BT-474 cells. A mutant T187A p27 was not phosphorylated, confirming that T187 is a Cdk2 phosphorylation site, as reported by Sheaff *et al.* (32).

Inhibition of the ErbB2 kinase also eliminated detectable P-MAPK in BT-474 cells (Fig. 4). Kawada *et al.* (33) showed that MAPK transfected into fibroblasts is capable of directly phosphorylating p27. Therefore, we precipitated MAPK from control and AG1478-treated cells and tested the immune complexes in kinase assays using MBP and p27 as substrates. Fig. 5*B* shows that MAPK from proliferating BT-474 cells phosphorylates MBP and p27 directly, whereas its activity is markedly reduced in cells arrested with AG1478. MAPK from proliferating cells was unable to phosphorylate T187A p27, suggesting that MAPK can also phosphorylate T187 directly. Cdk2 and cdc2 were not detectable in MAPK precipitates used to phosphorylate p27 *in vitro* (not shown), arguing against the presence of a known p27 kinase present in the MAPK precipitate. Because phosphorylation at T187 results in proteasome-mediated degradation of p27 (32, 34), we examined whether the inhibition ErbB2, by reducing Cdk2- and MAPK-mediated phosphorylation of p27, increased the stability of endogenous p27 using a modification of the method described by Loda *et al.* (25). In this method, the endogenous p27 is incubated at 30°C in the presence of ATP. Densitometric analysis of the p27 bands revealed a half-life of <3 h *versus* $\sim$6 h in proliferating *versus* quiescent, AG1478-treated cells, respectively.

Inhibition of ErbB2 Increases Nuclear Levels of p27 and Its Association with Nuclear Cdk2. We next evaluated how interruption of ErbB2 signaling with AG1478 affects the localization of cell cycle regulators. Fig. 6*A* shows that active MAPK (P-MAPK), Cdk4, and cyclin D1 reside mainly in the cytosol of untreated proliferating cells and are down-regulated by AG1478. In contrast, Cdk2, cyclin E, and total MAPK protein levels remain unaltered and can be found in both cytosol and cell nuclei. In proliferating cells, p27 is found in both compartments, where it coprecipitates with Cdk4 and Cdk2. Inhibition of the ErbB-2 kinase with AG1478 completely redirected p27 from cytosolic Cdk4 to nuclear Cdk2 (Fig. 6*B*), where it may inhibit Cdk2 activity (Fig. 5*B*) and mediate cell cycle arrest. Similar to Cdk2, cyclin E also associated at higher levels with p27 upon treatment with AG1478 (not shown).

ErbB2 Regulates the Transcription and Phosphorylation of Cyclin D1. Ras/MAPK and PI3K/Akt signaling have been implicated in the regulation of cyclin D1 (Ref. 35 and Refs. therein). Therefore, to study the role of these pathways in linking ErbB2 function to cyclin D1 regulation, we used LY294002 and U0126, specific inhibitors of the p110 catalytic subunit of PI3K and of MEK1/2, respectively. Fig. 7*A* confirms that AG1478 inhibited signaling through both MAPK and PI3K/Akt. However, LY294002 only affected PI3K signaling, as indicated by the complete inhibition of Ser-473 Akt and P-GSK-3β without affecting P-MAPK, whereas U0126 solely eliminated only P-MAPK. Nonetheless, both pathways seem to have some common targets. Cdk4 levels decreased upon inhibition of PI3K/Akt and MAPK, and the combined use of LY294002 and U0126 had a more

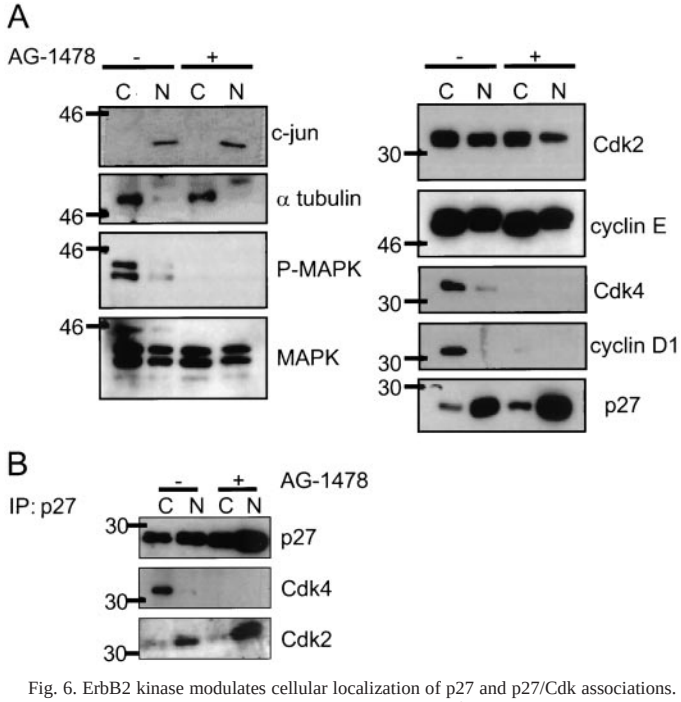

Fig. 6. ErbB2 kinase modulates cellular localization of p27 and p27/Cdk associations. Control and AG1478-treated (24 h) BT-474 cells were fractionated as described in "Materials and Methods." *A*, cytosolic (*C*) and nuclear (*N*) fractions were subjected to immunoblot analysis for P-MAPK, total MAPK, Cdk2, cyclin E, Cdk4, cyclin D1, and p27. c-jun and α-tubulin were used to confirm the nuclear and cytosolic fractions, respectively. *B*, 500 μg of cytosolic (*C*) and nuclear (*N*) fraction from treated and untreated BT-474 cells were precipitated with a p27 antibody and the immune complexes analyzed by p27, Cdk2, and Cdk4 immunoblot. *Left* of each *panel*, molecular weights in thousands.

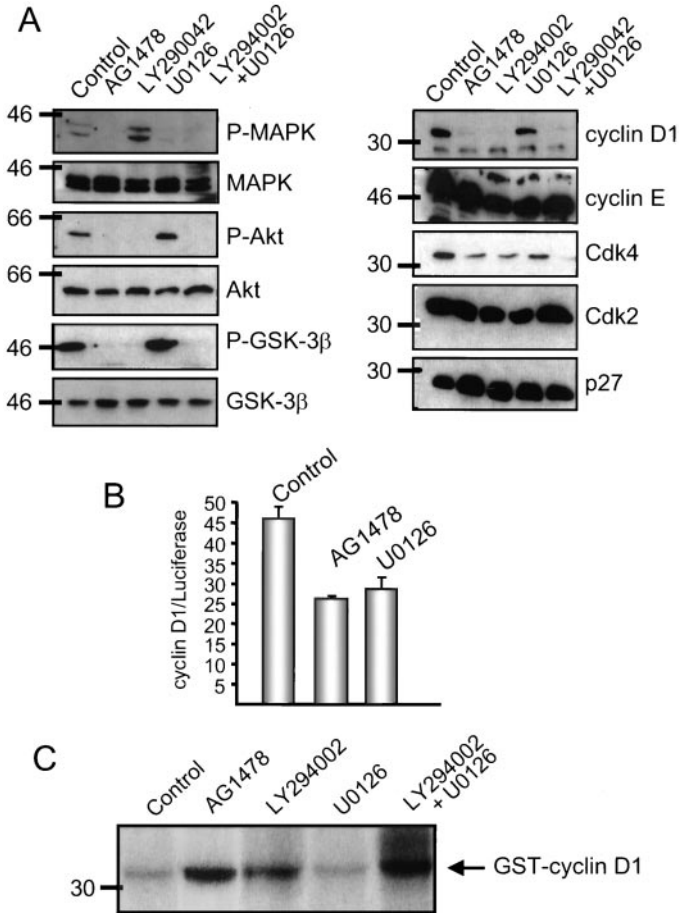

Fig. 7. Interruption of ErbB2 kinase activity reduces cyclin D1 by transcriptional and posttranslational mechanisms. *A*, cells were treated for 24 h with AG1478 (10 μM), LY294002 (40 μM), U0126 (5 μM), or both LY294002 and U0126. Total BT-474 cell protein (75 μg) was resolved by SDS-PAGE and subjected to immunoblot analyses for P-MAPK, MAPK, P-Akt, Akt, P-GSK-3β, GSK-3β, cyclin D1, cyclin E, Cdk2, Cdk4, and p27. *B*, cells were transiently transfected with a cyclin D1 Luc construct and incubated for 24 h with AG1478 (10 μM) or U0126 (5 μM). Promoter activity was measured using the Dual Luciferase Reporter Assay and expressed as "fold induction" compared with mock-transfected cells. Each *column* represents data generated from triplicate wells; *bars*, SD. *C*, GSK-3β was precipitated from BT-474 cells that had been treated for 24 h with the same specific inhibitors as in *A*. Immune complexes were tested for kinase activity against a GST-cyclin D1 fusion protein. Phosphorylated GST-cyclin D1 (M_r ~31,400) was visualized by autoradiography.

pronounced effect. Similar to AG1478, both LY294002 and U0126 up-regulated p27 levels. The levels of total Akt, total MAPK, total GSK-3β, cyclin E, and Cdk2 were not altered by any of the inhibitors.

Detectable cyclin D1 protein levels were eliminated by AG1478 and LY294002 but were modestly reduced by U0126 (Fig. 7*A*). We next investigated whether inhibition of ErbB2 signaling down-regulated cyclin D1 at a transcriptional level. BT-474 cells were transiently transfected with a cyclin D1/luciferase promoter construct and then treated with AG1478, LY294002, or U0126 for 24 h. Both AG1478 and U0126 (Fig. 7*B*) but not LY294002 reduced cyclin D1/luciferase expression ~50% compared with controls. The complete elimination of cyclin D1 by AG1478 and LY294002 (Fig. 7*A*) suggested that PI3K/Akt regulated cyclin D1 posttranscriptionally. To determine whether inhibition of PI3K/Akt resulted in GSK-3β-mediated phosphorylation of cyclin D1, we precipitated GSK-3β from BT-474 cells treated with different inhibitors and tested its activity *in vitro* against recombinant GST-cyclin D1. In untreated cells and cells treated with the MEK1/2 inhibitor, GSK-3β did not appreciably phosphorylate GST-cyclin D1 (Fig. 7*C*), consistent with the phosphorylated (inactive) GSK-3β protein detected by immunoblot (Fig. 7*A*). In contrast, in cells treated with AG1478, LY294002, or the combination of LY294002 plus U0126, GSK-3β was not phosphorylated (Fig. 7*A*) and, therefore, active and capable of phosphorylating cyclin D1 *in vitro* (Fig. 7*C*). Despite the different biochemical effects of LY294002 and U0126 when used alone, each was able to increase the G_1 fraction and reduce the S-phase fraction of BT-474 cells (Table 1), suggesting that both PI3-K/Akt and MAPK coordinately regulate ErbB2-driven tumor cell proliferation.

Cyclin D1 Overexpression Blocks AG1478-mediated Inhibition of Proliferation. To determine whether down-regulation of cyclin D1 played a role in the antiproliferative effect mediated by the ErbB inhibitor, we used an inducible cyclin D1 adenovirus. Forced expression of cyclin D1 expression in BT-474 cells resulted in Rb hyperphosphorylation, an increase in the basal S-phase fraction from 8 to 26%, and a modest increase in p27 levels but did not affect the ability of AG1478 to inhibit ErbB2 phosphorylation (Fig. 8). Addition of tet completely suppressed ectopic cyclin D1 expression. Under these conditions, the addition of AG1478 inhibited Rb phosphorylation, increased the G_1-phase fraction (75→82%), and reduced the S-phase fraction (8→3%). However, AG1478 had no effect in the absence of tet, indicating that an excess of cyclin D1 can negate the growth arrest resulting from inhibition of ErbB2.

Reduction of Cyclin D1/Cdk4 Precedes the Increase in p27 Levels. Cyclin D1 serves as the regulatory subunit of Cdk4 and contributes to its stability. In addition, cyclin D1/Cdk4 complexes can sequester cytosolic $p27^{Kip1}$ and titrate it away from Cdk2 (18, 36). Thus, low levels of cyclin D1 may potentially destabilize Cdk4 and indirectly contribute a larger amount of p27 available for Cdk2 binding. To determine whether the increase in p27 followed the down-regulation of cyclin D1 and Cdk4, we performed a time course in which BT-474 cells were exposed to AG1478 for up to 24 h. Fig. 9 shows rapid dephosphorylation (<2 h) of ErbB2, P-MAPK, P-Akt, and P-GSK-3β. After 6 h, detectable levels of cyclin D1 were eliminated, whereas Cdk4 remained stable for up to 12 h of exposure to AG1478. The increase in p27 was first detectable at 6 h, reaching a maximum at >24 h, the time at which an increase in G_1 and a reduction in S-phase were first detectable (Fig. 2). Although the levels of p27 were slightly variable in untreated BT-474 cells, no time-dependent increase in p27 protein levels occurred in the absence of AG1478. This temporal progression is consistent with a model in which the increase of p27 steady-state levels occurs as a consequence of the simultaneous inactivation of multiple ErbB2-modulated signaling inputs.

DISCUSSION

We have examined mechanisms by which ErbB2 signaling regulates cell cycle progression in BT-474 human breast carcinoma cells. These cells, which exhibit *ErbB2* gene amplification (27) and ~10^5 ErbB1 (EGFR) sites/cell (31), are ErbB2 dependent in that blockade of ErbB2 with antibodies against the receptor's ectodomain markedly inhibits their proliferation both *in vitro* and *in vivo* (37). ErbB2 is constitutively phosphorylated in BT-474 cells, suggesting that, in

Table 1 *Blockade of either PI3K/Akt or MAPK induces G_1 arrest of BT-474 cells*

Subconfluent BT-474 cells in IMEM/10% FCS were incubated with 10 μM AG1478, 40 μM LY294002, or 5 μM U0126. After 24 h, the cells were trypsinized, labeled with propidium iodide, and subjected to flow cytometric analysis.

Inhibitor	G_1	S	G_2-M
None	76	16	8
AG1478	89	4	7
LY294002	87	5	8
U0126	86	5	9

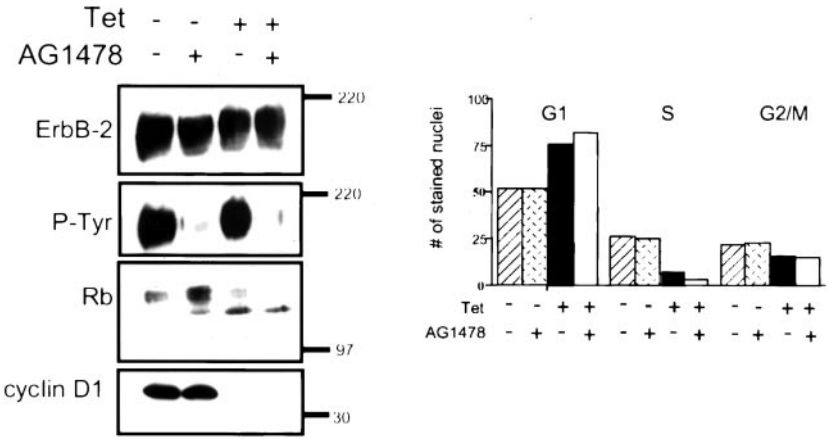

Fig. 8. Cyclin D1 overexpression negates the inhibitory effect of ErbB2 kinase inhibitor. Cells were infected with 200:1 viral particles of Ad-D1 and Ad-tTA as indicated in "Materials and Methods" and then incubated in IMEM/10% FCS ± 10 nM tet for 48 h. For the second 24 h, 5 μM AG1478 was added where indicated, after which cells were harvested and subjected to immunoblot or flow cytometric analysis. Each *lane* contains 50 μg of total protein. *Right side* of *left panel*, molecular weights in thousands.

these cells, the orphan receptor may be transactivated by ligand-activated EGFR. To block ErbB2 signaling, we used AG1478, a small molecule quinazoline inhibitor of the EGFR (ErbB1) kinase. In intact BT-474 cells, AG1478 inhibits the ErbB2 kinase and induces a reversible cell cycle arrest, thus providing a useful tool to study ErbB2-driven cell cycle progression. Although AG1478 is specific for the EGFR at submicromolar concentrations, several arguments support its use to block EGFR/ErbB2 cross-talk. It was shown that it induced the formation of inactive, unphosphorylated EGFR/ErbB2 heterodimers (29), conditions under which ErbB2 would be unable to interact with other ErbB coreceptors. We reported recently that AG1478 can suppress tumorigenesis in MMTV/*neu* + TGF-α bigenic mice (22), further suggesting that EGFR kinase inhibitors can inhibit tumor cell systems, such as BT-474 cells, in which the EGFR and ErbB2 (*neu*) cooperate. At the concentrations used, AG1478 had no effect against Cdk2 (38), MAPK (39), or Akt kinase[8] *in vitro*, implying that its effects on signaling pathways downstream of ErbB2 were not direct but secondary to its action at the receptor level.

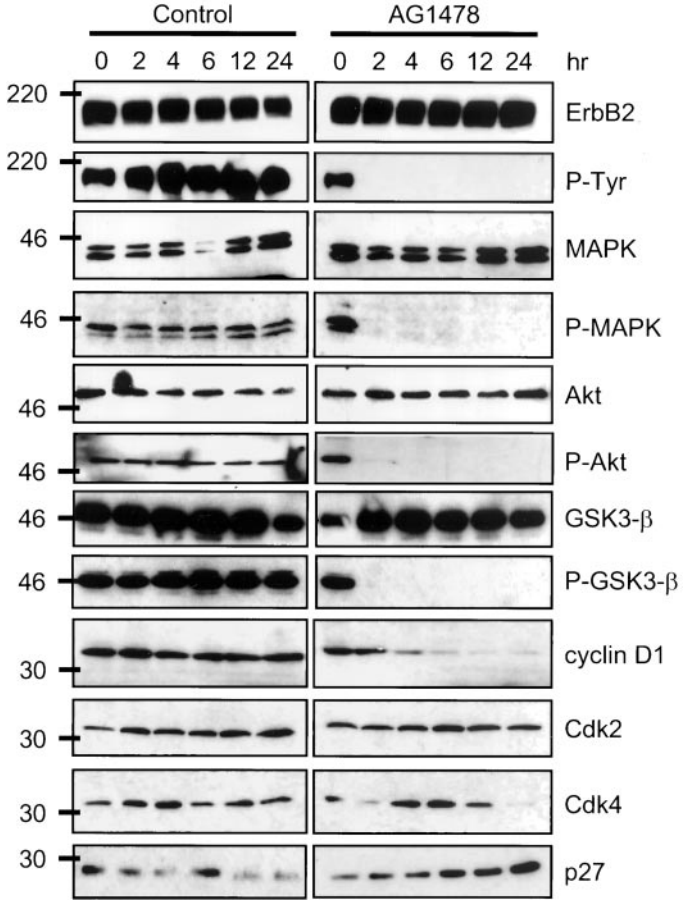

Fig. 9. Time course of changes in cell cycle regulatory molecules after inhibition of ErbB2 signaling. BT-474 cells were treated for 0, 2, 4, 6, 12, and 24 h with 10 μM AG1478. AG1478-treated cells and temporally matched untreated monolayers were harvested at the indicated times, lysed in EBC buffer, and subjected to immunoblot analyses using the indicated antibodies. *Left*, molecular weights in thousands.

Several reports link signaling pathways activated by ErbB2 with regulators of cell cycle progression. Activation of Ras/MAPK results in degradation of p27 and inhibits its ability to bind Cdk2 (33, 40). Both constitutive activation of MAPK (41) and overexpression of the ErbB2-homologous *neu* gene product (42) increase cyclin D1 transcription and expression. Via heterodimerization with ErbB3, ErbB2 can activate PI3K (3), which phosphorylates membrane phosphoinositides at the 3′ position of the inositol ring. These membrane-bound lipids recruit Akt, via its the pleckstrin homology domain, to the cell membrane, where this kinase is activated by phosphorylation in Thr-308 and Ser-473 by the 3-phosphoinositide-dependent protein kinases PDK1 and PDK2 (43). Akt can phosphorylate and negatively regulate GSK-3β, thereby inhibiting GSK-3β-mediated phosphorylation of cyclin D1 at Thr-286. This phosphorylation accelerates proteasome-mediated degradation of cyclin D1, thus shortening its half-life (26). Therefore, by activating MAPK and PI3K/Akt and indirectly disabling GSK-3β, an excess of ErbB2 signals can modulate cyclin D1 and p27 and dysregulate the G_1-to-S transition. Overexpression of ectopic ErbB2 in MCF-7 cells up-regulated both MAPK and PI3K/Akt activities and increased the turnover of endogenous p27. In these and in BT-474 cells, inhibition of the ErbB2 kinase with AG1478 blocked MAPK and Akt kinases and induced proliferation arrest, suggesting that both of these pathways are involved in ErbB2-driven cell cycle progression.

Although p27 can inhibit recombinant cyclin D1/Cdk4 complexes *in vitro*, it is more effective in antagonizing the activity of cyclin E/Cdk2 (16, 44). More recent data with primary mouse embryonic fibroblasts indicate that p27 can stabilize the assembly of cyclin D1/Cdk4 complexes and direct this heteromeric complex to the cell nucleus (36). On the other hand, in proliferating cells, cyclin D1/Cdk4 complexes can sequester p27 and limit p27 binding to and inhibition of cyclin E/Cdk2. Consistent with these studies, p27 was low and was associated at higher stoichiometry with Cdk4 than with Cdk2 in proliferating than in quiescent BT-474 cells. By reducing the amount of p27 available for Cdk2 binding, this association with cyclin D1/Cdk4 may indirectly facilitate Cdk2-mediated phosphorylation of p27 on T187 (Fig. 5*B*) to trigger its degradation. Similar results were reported recently by Lane *et al.* (45); growth arrest of proliferating

BT-474 cells with an inhibitory ErbB2 antibody completely redirected p27 from Cdk4 to Cdk2 complexes.

MAPK from BT-474 cells phosphorylated wild-type but not T187A p27, implying that this residue, similar to Cdk2, may also be a target for MAPK-mediated phosphorylation. This result, the shorter turnover of p27 in both MCF-7/ErbB2 clones compared with MCF-7/neo cells (Fig. 1) and in untreated *versus* AG1478-treated BT-474 cells (Fig. 5*C*), and the increase in steady-state p27 levels in BT-474 cells treated with the MEK1/2 inhibitor U0126 (Fig. 7*A*), all suggest that ErbB2-activated MAPK directly may contribute to the destabilization of p27. In addition, we showed that blockade of ErbB2 function with AG1478 inhibited the ability of BT-474 cell MAPK to phosphorylate p27 *in vitro* (Fig. 5*B*). This is unlikely because of a direct effect of AG1478 on Cdk2 because its *in vitro* IC_{50} against Cdk2 is >100 μM (38). Furthermore, we did not detect Cdk2 or cdc2, kinases well known to phosphorylate p27, in the MAPK precipitates used to phosphorylate p27 *in vitro*, suggesting that our result is not attributable to a contaminating p27-interacting kinase. This interaction of MAPK with T187 in p27 is not unique to BT-474 cells. We reported recently that MAPK precipitated from MMTV/*neu* + TGF-α tumors, in which the *neu* kinase is active, was able to phosphorylate wild-type but not T187A p27. In this same study, the ability of an MMTV/*neu* + TGF-α tumor lysate to degrade recombinant p27 *in vitro* was completely abrogated by the addition of U0126 (22). Bacterially expressed p27 has been shown to be exclusively phosphorylated on serine by GST-Erk1 *in vitro* (46). Ser-10 was reported recently as the major phosphorylation site of p27 *in vivo* (47). In this last study, however, Erk1/2 was unable to phosphorylate this site, arguing against the serine-exclusive phosphorylation of p27 by MAPK as reported by Alessandrini *et al.* (46). In a recent study, overexpression of HER2 in NIH-3T3 cells enhanced ubiquitin-mediated degradation and nuclear exclusion of p27, which were reduced by a dominant-negative Grb-2 mutant (48), further supporting a direct role for MAPK in the regulation of p27.

The previous data support the notion that MAPK-mediated destabilization of p27 contributes to ErbB2-driven cell cycle progression. However, it has been shown in mouse fibroblasts that activation of MEK1 is not sufficient *per se* to trigger the degradation of p27 unless cyclin D1 and Cdk4 subunits are co-overexpressed at levels achieved in cells stimulated by serum (18). These cyclin D1/Cdk4 complexes can then sequester untethered p27, reduce p27/Cdk2 stoichiometry and its inhibitory threshold of Cdk2, and thereby allow entry into S-phase. In the experimental system presented, this is supported by the high association of transduced cyclin D1 and endogenous p27 in highly proliferative BT-474 cells (Fig. 8). These data lead to the possibility that, in addition to destabilization of p27, other ErbB2-induced signals are required for progression into S-phase. On the other hand, one could argue that, in addition to the up-regulation of p27, the marked G_1 arrest after blockade of ErbB2 also requires the elimination of those additional proliferative signals.

The marked changes in cyclin D1/Cdk4 levels observed upon inhibition of ErbB2 support a critical role for this G1 cyclin in ErbB2-mediated cell cycle progression. Treatment of proliferating BT-474 cells with the MEK1/2 inhibitor U0126 inhibited cyclin D1 reporter activity while modestly reducing cyclin D1 protein levels (Fig. 7). On the other hand, treatment with the PI3K inhibitor LY294002 inhibited Akt activity, dephosphorylated GSK-3β, markedly reduced cyclin D1 levels, and enhanced the ability of cellular GSK-3β to phosphorylate cyclin D1 *in vitro* (Fig. 7). LY294002 did not inhibit MAPK activity in BT-474, suggesting that its effect on cyclin D1 was independent of an action on MAPK. AG1478, LY294002, and U0126 also down-regulated Cdk4, which followed the reduction of cyclin D1 (Figs. 7 and 9). Unassembled Cdk4 is known to turn over more rapidly and not accumulate (49). In addition, Erk (MAPK) activity has been shown to be required for cyclin D/Cdk4 assembly (18). Whether the reduction of cyclin D1 levels and/or MAPK activity can contribute to Cdk4 unassembly and destabilization requires further investigation outside the scope of this report. Nonetheless, the increase in p27 induced by each LY294002 and U0126 (Fig. 7*A*) could be secondary to the strong reduction in cyclin D1/Cdk4 complexes, which then leaves p27 untethered and able to stably bind Cdk2 at high stoichiometry (Fig. 6*B*), thus counteracting Cdk2-mediated phosphorylation and degradation of p27 (Fig. 5, *B* and *C*). These results suggest that ErbB2 may regulate cellular cyclin D1 at two molecular levels: (*a*) by transcriptional regulation via active MAPK; and (*b*) posttranslationally, via PI3K/Akt, by suppression of GSK-3β-mediated phosphorylation and subsequent degradation of cyclin D1. Reversal of these ErbB2-mediated effects on cyclin D1 may be required for the antiproliferative effect of AG1478 in B-474 cells. Induction of high levels of cyclin D1 prevented the cell cycle effects of the anti-ErbB small molecule (Fig. 8).

Both LY294002 and U0126 independently induce G_1 arrest and a 70% reduction in the S-phase fraction in BT-474 cells (Table 1), implying that both MAPK and PI3K are coordinately required for the dysregulated proliferation in ErbB2-overexpressing cells. A431 squamous cancer cells are highly dependent on autoactivated ErbB1 (EGFR) homodimers (50). A recent report suggested that in these cells, PI3K/Akt signaling but not MAPK was predominantly contributing to G_1-to-S progression (38). These different results with BT-474 and A431 cells suggest that different ErbB homo- or heterodimers may not rely on identical effector mechanisms for the subversion of the G_1-to-S transition. Notably, studies in (ErbB-null) 32D and BAF3 cells transfected with ectopic ErbB receptors, either singly or in combination (4, 51), have not addressed yet which molecules involved in the regulation of G_1-S are modulated by different ErbB dimers.

In summary, the data presented suggest that ErbB2 modulates cellular p27 and cyclin D1 protein levels through both Ras/MAPK and PI3K/Akt signaling. Reversible interruption of ErbB2 function, using a small molecule kinase inhibitor, inhibits MAPK (Erk) and reduces MAPK-mediated transcription of cyclin D1. In addition, PI3K/Akt signaling is inhibited, which relieves GSK-3β from Akt-mediated inhibitory phosphorylation, thus allowing GSK-3β to phosphorylate and degrade cyclin D1. The loss of Erk activity and cyclin D1 leave Cdk4 unassembled and possibly destabilize it. These events reduce the levels of cyclin D1/Cdk4 complexes that can sequester and titrate p27 away from binding to cyclin E/Cdk2 complexes and, in turn, inhibit Cdk2-mediated phosphorylation of Rb. Moreover, the inhibition of MAPK relieves p27 from MAPK-mediated phosphorylation on T187, further contributing to p27 stability and to its ability to bind to and inhibit Cdk2 function. In concert, these biochemical responses after ErbB2 blockade retain ErbB2-dependent cells in the G_1 phase of the cell cycle. The inability of ErbB2 inhibitors to elicit these responses may translate into resistance to ErbB2-targeted anticancer therapies.

REFERENCES

1. Gassmann, M., and Lemke, G. Neuregulins and neuregulin receptors in neural development. Curr. Opin. Neurobiol., *7:* 87–92, 1997.
2. Riese, D. J., II, and Stern, D. F. Specificity within the EGF family/ErbB receptor family signaling network. Bioessays, *20*: 41–48, 1998.
3. Yarden, Y., and Sliwkowski, M. X. Untangling the ErbB signalling network. Nat. Rev., *2:* 127–137, 2001.
4. Pinkas-Kramarski, R., Soussan, L., Waterman, H., Levkowitz, G. Alroy, I., Klapper, L., Lavi, S., Serger, R., Ratzkin, B. J., Sela, M., and Yarden, Y. Diversification of Neu differentiation factor and epidermal growth factor signalling by combinatorial receptor interactions. EMBO J., *15:* 2452–2467, 1996.
5. Karunagaran, D., Tzahar, E., Beerli, R. R., Chen, X., Graus-Porta, D., Ratzkin, B. J., Seger, R., Hynes, N. E., and Yarden, Y. ErbB2 is a common auxiliary subunit of NDF and EGF receptors: implications for breast cancer. EMBO J., *15:* 254–264, 1996.

6. Graus-Porta, D., Beerli, R. R., Daly, J. M., and Hynes, N. E. ErbB2, the preferred heterodimerization partner of all ErbB receptors, is a mediator of lateral signaling. EMBO J., *16:* 1647–1655, 1997.
7. Lenferink, A. E., Pinkas-Kramarski, R., van de Poll, M. L., van Vugt, M. J., Klapper, L. N., Tzahar, E., Waterman, H., Sela, M., van Zoelen, E. J., and Yarden, Y. Differential endocytic routing of homo- and hetero-dimeric ErbB tyrosine kinases confers signaling superiority to receptor heterodimers. EMBO J., *17:* 3385–3397, 1998.
8. Graus-Porta, D., Beerli, R., and Hynes, N. E. Single-chain antibody-mediated intracellular retention of ErbB2 impairs Neu differentiation factor and epidermal growth factor signaling. Mol. Cell. Biol., *15:* 1182–1191, 1995.
9. Qian, X., Dougall, W. C., Hellman, M. E., and Greene, M. I. Kinase-deficient neu proteins suppress epidermal growth factor function and abolish cell transformation. Oncogene, *9:* 1507–1514, 1994.
10. Hynes, N. E., and Stern, D. F. The biology of *ErbB2/neu/HER-2* and its role in cancer. Biochim. Biophys. Acta, *1198:* 165–184, 1994.
11. Elledge, S. J. Cell cycle checkpoints: preventing an identity crisis. Science (Wash. DC), *274:* 1664–1672, 1996.
12. Hunter, T., and Pines, J. Cyclins and cancer. II. Cyclin D and CDK inhibitors come of age. Cell, *79:* 1182–1191, 1994.
13. Sherr, C. J., and Roberts, J. M. CDK inhibitors: positive and negative regulators of G1-phase progression. Genes Dev., *13:* 1501–1512, 1999.
14. Yang, J., and Kornbluth, S. All aboard the cyclin train: subcellular trafficking of cyclins and their CDK partners. Trends Cell Biol., *9:* 207–210, 1999.
15. Sherr, C. J., and Roberts, J. M. Inhibitors of mammalian G1 cyclin-dependent kinases. Genes Dev., *9:* 1149–1163, 1995.
16. Polyak, K., Lee, M. H., Erdjument-Bromage, H., Koff, A., Roberts, J. M., Tempst, P., and Massagué, J. Cloning of p27, a cyclin-dependent kinase inhibitor and a potential mediator of extracellular antimitogenic signals. Cell, *78:* 59–66, 1994.
17. Toyoshima, H., and Hunter, T. p27, a novel inhibitor of G1 cyclin/cdk protein kinase activity, is related to p21. Cell, *78:* 67–74, 1994.
18. Cheng, M., Sexl, V., Sherr, C. J., and Roussel, M. F. Assembly of cyclin D-dependent kinase and titration of p27 regulated by mitogen-activated protein kinase kinase (MEK1). Proc. Natl. Acad. Sci. USA, *95:* 1091–1096, 1998.
19. Benz, C. C., Scott, G. K., Sarup, J. C., Johnson, R. M., Tripathy, D., Coronado, E., Shepard, H. M., and Osborne, C. K. Estrogen-dependent, tamoxifen-resistant tumorigenic growth of MCF-7 cells transfected with ErbB2/neu. Breast Cancer Res. Treat., *24:* 85–95, 1992.
20. Favata, M. F., Horiuchi, K. Y., Manos, E. J., Daulerio, A. J., Stradley, D. A., Feeser, W. S., Van Dyk, D. E., Pitts, W. J., Earl, R. A., Hobbs, F., Copeland, R. A., Magolda, R. L., Scherle, P. A., and Trzaskos, J. M. Identification of a novel inhibitor of mitogen-activated protein kinase kinase. J. Biol. Chem., *273:* 18623–18632, 1998.
21. Vlahos, C. J., Matter, W. F., Hui, K. Y., and Brown, R. F. A specific inhibitor of phosphatidylinositol 3-kinase, 2-(4-morpholinyl)-8-phenyl-4*H*-1-benzopyran-4-one (LY294002). J. Biol. Chem., *269:* 5241–5248, 1994.
22. Lenferink, A. E. G., Simpson, J. F., Shawver, L. K., Coffey, R. J., Forbes, J. T., and Arteaga, C. L. Blockade of the EGF receptor tyrosine kinase suppresses tumorigenesis in MMTV/Neu + MMTV/TGFα bigenic mice. Proc. Natl. Acad. Sci. USA, *97:* 9609–9614, 2000.
23. Flanagan, W. M., Wolf, J. J., Olson, P., Grant, D., Lin, K-Y., Wagner, R. W., and Matteucci, M. A cytosine analog that confers enhanced potency to antisense oligonucleotides. Proc. Natl. Acad. Sci. USA, *96:* 3513–3518, 1999.
24. Wroblewski, J. M., Yin, J., Wang, J., Hardy, S., and Meeker, T. C. An adenoviral vector encoding cyclin D1 induces cell cycle progression and apoptosis. Proc. Am. Assoc. Cancer Res., *39:* 252, 1998.
25. Loda, M., Cukor, B., Tam, S. W., Lavin, P., Fiorentino, M., Draetta, G. F., Jesup, J. M., and Pagano, M. Increased proteasome-dependent degradation of the cyclin-dependent kinase inhibitor in aggressive colorectal carcinomas. Nat. Med., *3:* 231–234, 1997.
26. Diehl, J. A., Cheng, M., Roussel, M. F., and Sherr, C. J. Glycogen synthase kinase-3β regulates cyclin D1 proteolysis and subcellular localization. Genes Dev., *12:* 3499–3511, 1998.
27. Alimandi, M. Romano, M., Curia, M. C., Muraro, R., Fedi, P., Aaronson, S. A., DiFiore, P. P., and Kraus, M. H. Cooperative signaling of ErbB3 and ErbB2 in neoplastic transformation and human mammary carcinomas. Oncogene, *10:* 1813–1821, 1995.
28. Levitzki, A., and Gazit, A. Tyrosine kinase inhibition: an approach to drug development. Science (Wash. DC), *267:* 1782–1788, 1995.
29. Arteaga, C. L., Ramsey, T. T., Shawver, L. K., and Guyer, C. A. Unliganded epidermal growth factor receptor dimerization induced by direct interaction of quinazolines with the ATP binding site. J. Biol. Chem., *272:* 23247–23254, 1997.
30. Arteaga, C. L. Hurd, S. D., Dugger, T. C., Winnier, A. R., and Robertson, J. B. Epidermal growth factor receptors in human breast carcinoma cells: a potential selective target for transforming growth factor α-*Pseudomonas* exotoxin 40 (TGFα-PE40) fusion protein. Cancer Res., *54:* 4703–4709, 1994.
31. Lewis, G. D., Figari, I., Fendly, B., Wong, W. L., Carter, P., Gorman, C., and Shepard, H. M. Differential responses of human tumor cell lines to anti-p185^{HER2} monoclonal antibodies. Cancer Immunol. Immunother., *37:* 255–263, 1993.
32. Sheaff, R., Groudine, M., Gordon, M., Roberts, J., and Sherr, C. J. Cyclin E-CDK2 is a regulator of p27Kip1. Genes Dev., *11:* 1464–1478, 1997.
33. Kawada, M., Yamagoe, S., Murakami, Y., Suzuki, K., Mizuno, S., and Uehara, Y. Induction of p27 degradation and anchorage independence by Ras through the MAP kinase signaling pathway. Oncogene, *15:* 629–637, 1997.
34. Vlach, J., Hennecke, S., and Amati, B. Phosphorylation-dependent degradation of the cyclin-dependent kinase inhibitor p27. EMBO J., *16:* 5334–5344, 1997.
35. Malumbres, A., and Pellicer, A. Ras pathways to cell cycle control and cell transformation. Front. Biosci., *3:* d887–d912, 1998.
36. Cheng, M., Olivier, P., Diehl, J. A., Fero, M., Roussel, M. F., Roberts, J. M., and Sherr, C. J. The p21 and p27 CDK "inhibitors" are essential activators of cyclin D-dependent kinases in murine fibroblasts. EMBO J., *18:* 1571–1583, 1999.
37. Baselga, J., Norton, L., Albanell, J., Kim, Y-M., and Mendelsohn, J. Recombinant humanized anti-HER2 antibody (Herceptin) enhances the antitumor activity of paclitaxel and doxorubicin against HER2/*neu* overexpressing human breast cancer xenografts. Cancer Res., *58:* 2825–2831, 1998.
38. Busse, D., Doughty, R. S., Ramsey, T. T., Russell, W. E., Price, J. O., Flanagan, W. M., Shawver, L. K., and Arteaga, C. L. Reversible G1 arrest induced by inhibition of the epidermal growth factor receptor tyrosine kinase requires up-regulation of p27 independent of MAPK activity. J. Biol. Chem., *275:* 6987–6995, 2000.
39. Kurokawa, H., Lenferink, A. E. G., Simpson, J. F., Pisacane, P. I., Sliwkowski, M. X., Forbes, J. T., and Arteaga, C. L. Inhibition of HER2/*neu* (*erb*B-2) and mitogen-activated protein kinases enhances tamoxifen action against HER2-overexpressing, tamoxifen-resistant breast cancer cells. Cancer Res., *60:* 5887–5894, 2000.
40. Rivard, N., Boucher, M.-J., Asselin, C., and L'Allemain, G. MAP kinase cascade is required for p27 downregulation and S phase entry in fibroblasts and epithelial cells. Am. J. Physiol., *277:* C652–C664, 1999.
41. Lavoie, J. N., L'Allemain, G., Brunet, A., Muller, R., and Pouyssegur, J. Cyclin D1 expression is regulated positively by the p42/p44MAPK and negatively by the p38/HOGMAPK pathway. J. Biol. Chem., *271:* 20608–20616, 1996.
42. Lee, R. J., Albanese, C., Fu, M., D'Amico, M., Lin, B., Watanabe, G., Haines, G. K., III, Siegel, P. M., Hung, M-C., Yarden, Y., *et al.* Cyclin D1 is required for transformation by activated neu and is induced through and E2F-dependent signaling pathway. Mol. Cell. Biol., *20:* 672–683, 2000.
43. Datta, S. R., Brunet, A., and Greenberg, M. E. Cellular survival: a play in three Akts. Genes Dev., *13:* 2905–2927, 1999.
44. LaBaer, J., Garrett, M. D., Stevenson, L. F., Slingerland, J. M., Sandhu, C., Chou, H. S., Fattaey, A., and Harlow, E. New functional activities for the p21 family of CDK inhibitors. Genes Dev., *11:* 847–862, 1997.
45. Lane, H. A., Beuvink, I., Motoyama, A. B., Daly, J. M., Neve, R. M., and Hynes, N. E. ErbB2 potentiates breast tumor proliferation through modulation of p27-Cdk2 complex formation: receptor overexpression does not determine growth dependency. Mol. Cell. Biol., *20:* 3210–3223, 2000.
46. Alessandrini, A., Chiaur, D. S., and Pagano, M. Regulation of the cyclin-dependent kinase inhibitor p27 by degradation and phosphorylation. Leukemia (Baltimore), *11:* 342–345, 1997.
47. Ishida, N., Kitagawa, M., Hatakayama, S., and Nakayama, K-i. Phosphorylation at serine 10, a major phosphorylation site of p27^{Kip1}, increases its protein stability. J. Biol. Chem., *275:* 25146–25154, 2000.
48. Yang, H-Y., Zhou, B. P., Hung, M-C., and Lee, M-H. Oncogenic signals of HER-2/*neu* in regulating the stability of the cyclin-dependent kinase inhibitor p27. J. Biol. Chem., *275:* 24735–24739, 2000.
49. Stepanova, L., Leng, X., Parker, S. B., and Harper, J. W. Mammalian p50^{Cdc37} is a protein kinase-targeting subunit of Hsp90 that binds and stabilizes Cdk4. Genes Dev., *10:* 1491–1502, 1996.
50. Van de Vijver, M., Kumar, R., and Mendelsohn, J. Ligand-induced activation of A431 cell epidermal growth factor receptors occurs primarily by an autocrine pathway that acts upon receptors on the surface rather than intracellularly. J. Biol. Chem., *266:* 7503–7508, 1991.
51. Riese, D. J., van Raaij, T. M., Plowman, G. D., Andrews, G. C., and Stern, D. F. The cellular response to neuregulins is governed by complex interactions of the ErbB receptor family. Mol. Cell. Biol., *15:* 5770–5776, 1995.